Title

Maternal-to-zygotic transition as a potential target for niclosamide during early embryogenesis

Authors

Vliet, Sara MF
Dasgupta, Subham
Sparks, Nicole RL
et al.

Publication Date

2019-10-01

DOI

10.1016/j.taap.2019.114699

Peer reviewed

HHS Public Access

Author manuscript

Toxicol Appl Pharmacol. Author manuscript; available in PMC 2020 October 01.

Published in final edited form as:

Toxicol Appl Pharmacol. 2019 October 01; 380: 114699. doi:10.1016/j.taap.2019.114699.

Maternal-to-Zygotic Transition as a Potential Target for Niclosamide During Early Embryogenesis

Sara M.F. Vliet[a,b], **Subham Dasgupta**[b], **Nicole R.L. Sparks**[c], **Jay S. Kirkwood**[d], **Alyssa Vollaro**[d], **Manhoi Hur**[d], **Nicole I. zur Nieden**[c], **David C. Volz**[b,*]

[a]Environmental Toxicology Graduate Program, University of California, Riverside, CA, USA

[b]Department of Environmental Sciences, University of California, Riverside, CA, USA

[c]Department of Molecular, Cell, and Systems Biology, University of California, Riverside, CA, USA

[d]Metabolomics Core Facility, Institute for Integrative Genome Biology, University of California, Riverside, CA, USA

Abstract

Niclosamide is an antihelminthic drug used worldwide for the treatment of tapeworm infections. Recent drug repurposing screens have highlighted the broad bioactivity of niclosamide across diverse mechanisms of action. As a result, niclosamide is being evaluated for a range of alternative drug-repurposing applications, including the treatment of cancer, bacterial infections, and Zika virus. As new applications of niclosamide will require non-oral delivery routes that may lead to exposure *in utero*, it is important to understand the mechanism of niclosamide toxicity during early stages of embryonic development. Previously, we showed that niclosamide induces a concentration-dependent delay in epiboly progression in the absence of effects on oxidative phosphorylation – a well-established target for niclosamide. Therefore, the overall objective of this study was to further examine the mechanism of niclosamide-induced epiboly delay during zebrafish embryogenesis. Based on this study, we found that (1) niclosamide exposure during early zebrafish embryogenesis resulted in a decrease in yolk sac integrity with a concomitant decrease in the presence of yolk sac actin networks and increase in cell size; (2) within whole embryos, niclosamide exposure did not alter non-polar metabolites and lipids, but significantly altered amino acids specific to aminoacyl-tRNA biosynthesis; (3) niclosamide significantly altered transcripts related to translation, transcription, and mRNA processing pathways; and (4) niclosamide did not significantly alter levels of rRNA and tRNA. Overall, our findings suggest that niclosamide may be causing a systemic delay in embryonic development by disrupting the

*Corresponding author. david.volz@ucr.edu.

Declaration of interests

The authors declare that they have no known competing financial interests or personal relationships that could have appeared to influence the work reported in this paper.

The authors declare the following financial interests/personal relationships which may be considered as potential competing interests:

translation of maternally-supplied mRNAs, an effect that may be mediated through disruption of aminoacyl-tRNA biosynthesis.

Keywords

zebrafish; maternal-to-zygotic transition; embryonic development; niclosamide

1. Introduction

Niclosamide (2',5-dichloro-4-nitro salicylanilide) is an oral antihelminthic drug that is approved by the U.S. Food and Drug Administration and has been used since the 1960s for the treatment of intestinal parasites, such as tapeworm, in humans and animals (Andrews et al., 1982). The antiparasitic activity of niclosamide is thought to be mediated through disruption of mitochondrial oxidative phosphorylation (OXPHOS) and inhibition of ATP production (Weinbach and Garbus, 1969), a hypothesis based on a number of studies that identified uncoupling activity of niclosamide in isolated mitochondria and invertebrates (Raheem et al., 1980; Tao et al., 2014; Yorke and Turton, 1974)

Beyond its traditional use in public health and veterinary medicine, niclosamide has recently received attention as a promising drug repurposing candidate for the potential treatment of a broad range of conditions including cancer (Chen et al., 2017; Pan et al., 2012), bacterial infections (Imperi et al., 2013; Tharmalingam et al., 2018), endometriosis (Prather et al., 2016), and Zika virus (Cairns et al., 2018; Li et al., 2017; Xu et al., 2016). Although the mechanisms underlying many of these alternative uses remains unclear, these studies have reported that niclosamide can interact with a wide range of signaling pathways including NF-κβ, Wnt/ß-catenin, NLRP3, STAT3, mTORC1, Notch, and LC3 lipidation (Balgi et al., 2009; Chen et al., 2009; Domalaon et al., 2019; Jin et al., 2010; Liu et al., 2019; Mook et al., 2019; Newton, 2019; Ren et al., 2010; Suliman et al., 2016; Tran and Kitami, 2019). The broad bioactivity of niclosamide across diverse biochemical pathways raises questions about its specificity as an OXPHOS uncoupler and suggests that mechanisms underlying potential therapeutic effects may be complex.

As an antihelminthic drug, niclosamide is administered orally and is generally well-tolerated, demonstrating very low toxicity and minimal side effects (EPA, 1999). This is due, in part, to niclosamide's low oral bioavailability and rapid metabolism within the gastrointestinal tract (Espinosa-Aguirre et al., 1991), a chemical feature that makes it ideal for treatment of intestinal parasites but, on the other hand, may prove challenging within many of the proposed off-label uses. To address this challenge, new formulations of niclosamide or non-oral routes of exposure will likely be required to maintain efficacy within the context of unconventional uses (Li et al., 2014; Lu et al., 2016). Considering this need for alternative drug delivery along with the wide range of observed bioactivity, a further understanding of the potential toxicity of niclosamide is necessary.

Previous work in our lab has highlighted the potential for developmental toxicity following niclosamide exposure during early embryogenesis (Vliet et al., 2018). Using embryonic stages of zebrafish as a model for early development, we demonstrated that exposure to low

micromolar concentrations of niclosamide results in a concentration-dependent delay in epiboly during gastrulation, a key developmental process that involves spreading of the embryonic cell mass around the yolk sac. Moreover, we found that niclosamide did not affect embryonic oxygen consumption, suggesting that oxidative phosphorylation may not play a role in niclosamide-induced epiboly delay. However, mRNA-sequencing revealed that niclosamide may be delaying the progression of epiboly by disrupting the timing of zygotic genome activation, an effect that may be mediated through effects on maternal transcriptional processes and/or the formation of cytoskeletal actin networks (Vliet et al., 2018).

Activation of the zygotic genome – and subsequent degradation of maternally-supplied mRNA – is a key developmental landmark that is conserved across vertebrate species, although the precise timing of this transition varies by species (Sha et al., 2019; Yartseva and Giraldez, 2015). Regardless of when it occurs, the maternal-to-zygotic transition (MZT) is critical for normal embryonic development (Duffie and Bourc'his, 2013; Langley et al., 2014; Li et al., 2013). In addition to the MZT, the presence of an intact cytoskeleton network is also required for proper cell division, cell migration, and progression of embryonic development (Cheng et al., 2004; Gallicano, 2001; Solnica-Krezel, 2005; Solnica-Krezel and Driever, 1994). Given the importance of the MZT and cytoskeletal networks in embryonic development across species, additional studies are needed to understand how niclosamide may disrupt these early developmental processes. Therefore, using zebrafish embryos and human embryonic stem cells as model systems, the overall objective of this study was to investigate the mechanism of toxicity of niclosamide.

2. Materials and Methods

2.1 Animals

Adult wildtype (strain 5D) zebrafish were maintained and bred on a recirculating system using previously described procedures (Vliet et al., 2017). For all experiments, newly fertilized eggs were collected within 30 min of spawning, rinsed, and reared in a temperature-controlled incubator at 28°C under a 14:10-h light-dark cycle. All embryos were sorted and staged according to previously described methods (Kimmel et al., 1995). All adult breeders were handled and treated in accordance with an Institutional Animal Care and Use Committee (IACUC)-approved animal use protocols (#20150035 and #20180063) at the University of California, Riverside.

2.2 Chemicals

Niclosamide (≥98% purity) was purchased from Sigma-Aldrich (St. Louis, MO, USA). Stock solutions were prepared in high performance liquid chromatography (HPLC)-grade dimethyl sulfoxide (DMSO) and stored within 2-mL amber glass vials with polytetrafluoroethylene-lined caps. Working solutions were prepared in particulate-free water from our recirculating system (pH and conductivity of ~7.2 and ~950 μS, respectively) immediately prior to each experiment, resulting in 0.1% DMSO within all vehicle control and treatment groups.

2.3 Whole-Mount Immunohistochemistry

Embryos (10 embryos per petri dish; three replicate petri dishes per treatment) were exposed under static conditions at 28°C from 2 to 5 hpf to either vehicle (0.1% DMSO) or niclosamide (0.313 μM) – a concentration that reliably induces epiboly delay in zebrafish (Vliet et al., 2018). At 5 hpf, embryos were removed from treatment solution, individual treatment dishes pooled (30 per pool; three replicate pools) and fixed overnight in 4% paraformaldehyde/1X phosphate buffered saline (PBS). Following fixation, embryos were manually dechorionated, rinsed, and incubated overnight in a 1:200 dilution of fluorescein-labelled phalloidin (ThermoFisher Scientific, Waltham, MA, USA). Stained embryos were imaged using a Leica MZ10 F stereomicroscope equipped with a DMC2900 camera. Actin fluorescence localized within the yolk sac was quantified within Adobe Photoshop. The yolk sac was selected manually – from immediately below the cell mass boundary to the vegetal pole – for each embryo and a color mask was created by selecting the stained area in control embryos. Average cell area was determined by manually tracing 10 randomly selected cells on each embryo (50 total embryos), resulting in a total of 500 measurements.

2.4 Whole-Embryo Metabolomics

To extract metabolites from zebrafish embryos, 500 μL of ice-cold solvent (30:30:20:20 MeOH:ACN:IPA:water) was added to pools of 30 embryos. Samples were then sonicated 15 min, vortexed 15 min, sonicated 15 min, then centrifuged at 16,000 × g at 4°C for 15 min. Supernatant was transferred to glass HPLC vials for LC-MS analysis.

Untargeted non-polar metabolomics was performed on a Xevo G2-XS quadrupole time-of-flight mass spectrometer (Waters, Milford, MA, USA) coupled to an H-class UPLC system (Waters, Milford, MA, USA). Separations were carried out on a CSH C18 column (2.1 × 100 mm, 1.7 μM) (Waters, Milford, MA, USA). The mobile phases were (A) 60:40 acetonitrile:water with 10 mM ammonium formate and 0.1% formic acid and (B) 90:10 isopropanol:acetonitrile with 10 mM ammonium formate and 0.1% formic acid. The flow rate was 350 μL/min and the column was held at 50°C. The injection volume was 1 μL. The following gradient program (with respect to mobile phase B) was used: 0–1 min, 10% B; 1–3 min, 20%, 3–5 min, 40% B; 5–16 min, 80% B; 16–20 min 99% B; 20–20.5 min, 10% B. Prior to LC-MS analysis, samples were diluted 40-fold to prevent detector saturation. The MS was operated in positive ion mode (50 to 1200 m/z) with a 100 ms scan time. Source and desolvation temperatures were 120° C and 500°C, respectively. Desolvation and cone gas were set to 1000 and 150 L/hr., respectively. All gases were nitrogen except the collision gas (argon). Capillary voltage was 1 kV. A quality control sample, generated by pooling equal aliquots of each sample, was analyzed every 4–5 injections to monitor system stability and performance. Samples were analyzed in random order. Leucine enkephalin was infused and used for mass correction.

Targeted polar metabolomics was performed on a TQ-XS triple quadrupole mass spectrometer (Waters, Milford, MA, USA) coupled to an I-class UPLC system (Waters, Milford, MA, USA). Separations were carried out on a ZIC-pHILIC column (2.1 × 150 mm, 5 μM) (EMD Millipore). The mobile phases were (A) water with 15 mM ammonium bicarbonate adjusted to pH 9.6 with ammonium hydroxide and (B) acetonitrile. The flow

rate was 200 μL/min and the column was held at 50°C. The injection volume was 1 μL. The following gradient program (with respect to mobile phase B) was used: 0–16 min, 90% B; 16–18 min, 20% B; 18–28 min, 90% B. The MS was operated in selected reaction monitoring mode. Source and desolvation temperatures were 150°C and 500°C, respectively. Desolvation and cone gases were set to 1000 and 150 L/hr., respectively. Collision gas was set to 0.15 mL/min. All gases were nitrogen except the collision gas (argon). Capillary voltage was 1 kV in positive ion mode and 2 kV in negative ion mode. A quality control sample, generated by pooling equal aliquots of each sample, was analyzed every 4–5 injections to monitor system stability and performance. Samples were analyzed in random order.

Data processing (peak picking, alignment, deconvolution, integration, normalization, and spectral matching) for untargeted non-polar metabolomics was performed in Progenesis Qi software (Nonlinear Dynamics, Durham, NC, USA). Data were normalized to total ion abundance. Features with a coefficient of variation (CV) greater than 20% or with an average abundance less than 200 in the quality control injections were removed (Dunn et al., 2011). To help identify features that belong to a single metabolite, features were assigned a cluster ID using RAMClust (Broeckling et al., 2014). An extension of the metabolomics standard initiative guidelines was used to assign annotation level confidence (Schymanski et al., 2014; Sumner et al., 2007). Several MS/MS metabolite databases were searched against including Metlin, Mass Bank of North America, Lipidblast, and an in-house database. Data for targeted polar metabolomics were processed and peaks integrated with the open source software Skyline (https://skyline.ms) (MacLean et al., 2010). Q values were generated by performing the Benjamini-Hochberg correction of *p*-values generated from an ANOVA in R using the aov function.

2.5 Whole-Embryo mRNA-Sequencing

Data from our prior mRNA-sequencing experiments (Vliet et al., 2018) were used to determine potential effects on the transcriptome within zebrafish embryos treated with 0.313 μM niclosamide from 2–3 and 2–5 hpf, as transcriptome-wide differential expression analysis was not previously conducted, and prior data were solely used for read-count analysis. Raw Illumina (fastq.gz) sequencing files (36 files totaling 8.24 GB) are available via NCBI's BioProject database under BioProject ID PRJNA454154, and all data were processed as previously described (Vliet et al., 2018). A DESeq2 application within Bluebee (Lexogen Quantseq DE 1.2) was used to identify significant treatment-related effects on transcript abundance (relative to vehicle controls) based on a false discovery rate (FDR) *p*-adjusted value < 0.05. Using DESeq2-identified transcripts, significantly altered genes were examined for enrichment of known biological processes and KEGG pathways using DAVID v6.8 (Dennis et al., 2003; Huang et al., 2009a, 2009b). Identification of maternal vs. zygotic transcripts was conducted following previously published methods (Vliet et al., 2018).

2.6 Whole-Embryo rRNA and tRNA Analysis

To determine the relative contribution of ribosomal RNA (rRNA) and transfer RNA (tRNA), total RNA samples from embryos exposed to either niclosamide (0.313 μM) or vehicle control (0.1% DMSO) from 2–3 and 2–5 hpf were analyzed on an Agilent 2100 Bioanalyzer

system (Santa Clara, CA). Peaks corresponding to 5.0S, 5.8S, 18S, 28S, and tRNA were integrated to determine RNA concentration. tRNA and rRNA concentrations were then normalized to total RNA concentrations to determine percent contribution.

2.7 Human Embryonic Stem Cell Exposure & Immunocytochemistry

Human embryonic stem cells (hESCs) of the H9 line were acquired from WiCell Research Institute (Madison, WI, USA), cultured on Matrigel-treated dishes (BD Biosciences, La Jolla, CA, USA), and maintained as feeder-free cultures in mTeSR media (Stem Cell Technologies, Vancouver, Canada) in 5% CO_2 at 37°C. Pluripotent colonies were passaged every five days upon reaching 70% confluency by dissociating cells with Accutase and a cell scraper. Differentiation was induced from confluent hESC cultures by switching to spontaneous differentiation medium consisting of Dulbecco's Modified Eagle's Medium (ThermoFisher Scientific, Waltham, MA, USA), 15% fetal bovine serum (Atlanta Biologicals, Flowery Branch, GA, USA), 1% non-essential amino acids (ThermoFisher Scientific, Waltham, MA, USA), 1:200 penicillin/streptomycin (ThermoFisher Scientific, Waltham, MA, USA), and 0.1 mM β-mercaptoethanol (Sigma-Aldrich, St. Louis, MO, USA). Niclosamide exposures were performed for the first 24 or 48 h of differentiation with nine concentrations ranging from 0.01 to 10 μM. A solvent control containing 0.1% DMSO was included to control for non-chemical specific effects.

Cellular survival in response to niclosamide treatment was determined with 3-[4,5-dimethylthiazol-2-yl]-2,5-diphenylterazolium bromide (MTT) (Spectrum Chemicals, Gardena, CA, USA). Briefly, MTT solution was added to cell media to a final concentration of 0.5 mg/ml and incubated at 37°C. After 2 h, the medium/MTT mix was replaced with pre-warmed MTT desorption solution (0.7% sodium dodecyl sulfate, SDS) in 2-propanol and cells were gently rocked for 15 min. The change in absorbance was read at 570 nm using an iMark microplate reader (Bio-Rad, Hercules, CA, USA). As the generation of blue formazan product is proportional to dehydrogenase activity, a decrease in absorbance at 570 nm provided a direct measurement of the number of viable cells. For concentrations of niclosamide that did not result in significant effects on cell viability across both time-points (≥1.0 μM), hESCs were fixed by incubating in 4% PFA for 20 min at 4°C. Following incubation, cells were washed 3 times in 1X PBS for 5 min. Cells were then stored at 4°C in 1X PBS until staining. Fixed cells were permeabilized by incubation in 150 μL of 0.1% Triton X-100 in 1X PBS for 15 min at room temperature. Cells were then washed three times for 5 minutes in 150 μL 1X PBS and incubated overnight at 4°C in a 1:150 dilution of fluorescein-labelled phalloidin (ThermoFisher Scientific, Waltham, MA, USA). Cells were then counterstained with DAPI by incubating in a 1:3 dilution of Fluoromount-G (SouthernBiotech, Birmingham, AL, USA). Cells were then washed three times for 5 min in 200 μL 1X PBS and stored in 300 μL 1X PBS at 4°C until imaged. Cells were imaged on our ImageXpress Micro XLS Widefield High-Content Screening System (Molecular Devices, Sunnyvale, CA, USA). Briefly, a 10X objective and DAPI/FITC filter cubes were used to acquire a z-stack (10 steps, 5 μM per step) of 56 sites per each well. Z-stack slices were used to generate a two-dimensional projection of each site, and sites were then stitched together within MetaXpress 6.0.3.1658 (Molecular Devices, Sunnyvale, CA, USA) to

generate a single image of the entire well. Actin networks within each well were quantified by measuring total FITC fluorescence per well within ImageJ (v1.51m9).

2.8 Statistical Analysis

All statistical analyses were performed using Prism 8 (GraphPad, San Diego, CA, USA). For all data not specified otherwise, main effects of treatment were identified using a one-way ANOVA (α=0.05). Treatment groups were compared with either time- or stage-matched (phenotype-based) vehicle controls using pair-wise Tukey-based multiple comparisons of least square means to identify significant differences among treatment groups (α=0.05).

3. Results

3.1 Embryonic Yolk Sac Integrity, Cell Area, and Actin Networks

To determine if niclosamide-induced developmental delays were due to abnormal formation of embryonic actin networks, we exposed embryos to 0.313 μM niclosamide from 2–5 hpf followed by fluorescent labeling of actin networks. Interestingly, niclosamide-exposed embryos were, following fixation, significantly more fragile relative to vehicle controls, resulting in a loss of yolk sac integrity (Figure 1A). Moreover, actin fluorescence localized to the embryonic yolk sac was significantly decreased within niclosamide-exposed embryos relative to vehicle controls, suggesting that niclosamide may be delaying the progression of yolk sac cortical actin networks (Figure 1B). Finally, niclosamide exposure resulted in a significant increase in average cell area in the blastomere (Figure 1C). As progressive reductions in cell size is associated with successive cell divisions, these data suggest that niclosamide exposure may also delay proliferation of cells within the embryonic blastomere. Exposure to niclosamide did not affect the formation of cellular actin networks within hESCs (Figure S1), suggesting that factors absent within hESCs may be driving actin-related effects observed within zebrafish embryos.

3.2 Whole-Embryo Metabolomics

As early embryonic development in zebrafish is dependent, in part, on uptake of maternally deposited nutrients in the yolk as well as metabolism of cellular lipid droplets (Dutta and Sinha, 2017), we investigated the metabolomic profiles of zebrafish embryos following niclosamide exposure. The abundance and distribution of non-polar metabolites and lipids were not significantly affected within embryos exposed to 0.313 μM niclosamide from 2–5 hpf (Figures 2A and 2B; Supplementary Data S1). However, niclosamide exposure resulted in significant alterations on polar metabolites, where the majority of significantly affected metabolites were amino acids involved in the aminoacyl-tRNA biosynthesis pathway (Figures 3A and 3B; Figure 4; Supplementary Data S1). These results suggest that, within embryos exposed from 2–5 hpf, niclosamide affected the abundance and distribution of amino acids in the absence of effects of non-polar metabolites and lipids.

3.3 Whole-Embryo mRNA-Sequencing

To further understand the mechanism of niclosamide-induced epiboly delay during early zebrafish embryogenesis, we leveraged prior mRNA-sequencing data generated from zebrafish exposed to niclosamide from 2–3 and 2–5 hpf, and then analyzed these data to

identify potential transcriptome-wide differences, an analysis that was not conducted in our prior study (Vliet et al., 2018). Exposure to niclosamide from 2–5 hpf resulted in significant alterations to 1) 1,526 transcripts relative to time-matched (2–5 hpf) vehicle controls (Figure 5A; Supplementary Data S1) and 2) 98 transcripts relative to stage-matched (2–3 hpf) vehicle controls (Figure 5B; Supplementary Data S1).

Of the significantly altered transcripts, 64 were shared between time- and stage-matched comparisons (Supplementary Data S1). Interestingly, of these shared transcripts, the majority were decreased and increased when compared to time- and stage-matched controls, respectively. Relative to time-matched (2–5 hpf) vehicle controls, significantly altered transcripts within niclosamide-exposed embryos were grouped within the spliceosome pathway and related to biological processes involved in transcription, phosphorylation, and multicellular development (Figure 6). Relative to stage-matched (2–3 hpf) vehicle controls, significantly altered transcripts were grouped within the ribosome pathways and related to biological processes involved in translation, among other processes (Figure 6).

3.4 Whole-Embryo rRNA and tRNA Analysis

To further understand how niclosamide may potentially be interacting with translational machinery, we quantified levels of ribosomal RNA and transfer RNA within total RNA samples of embryos exposed to either niclosamide (0.313 μM) or vehicle control (0.1% DMSO) from either 2–3 or 2–5 hpf. No significant alterations in the relative abundance of rRNA of tRNA were observed across either treatment condition or timepoint (Figure 7A and 7B), suggesting that niclosamide is not directly impacting the synthesis or recycling of these RNA species.

4. Discussion

In our prior study, niclosamide was shown to result in a concentration-dependent delay in epiboly progression during early zebrafish embryogenesis, an effect that may not be a result of OXPHOS disruption (Vliet et al., 2018). Due to the critical role of cytoskeletal networks in epiboly progression and the presence of altered cytoskeleton transcripts following niclosamide exposure (Lepage and Bruce, 2010; Solnica-Krezel and Driever, 1994; Vliet et al., 2018), we initially hypothesized that niclosamide delays epiboly progression through disruption of the embryonic cytoskeleton. Although no alterations in the abundance nor localization of tubulin were previously observed (Vliet et al., 2018), in the present study we demonstrated that exposure to niclosamide during early zebrafish embryogenesis significantly decreased yolk sac integrity relative to vehicle controls. During this stage of zebrafish embryogenesis, the structural integrity of the yolk sac is thought to be supported by a dense area of filamentous actin at the vegetal pole that maintains embryonic morphology (Cheng et al., 2004; Lepage and Bruce, 2010). The presence of this network is important during the late-blastula and early-gastrula stage of development when major cell rearrangements occur and the yolk cell is subjected to a number of physical forces (Keller et al., 2003). Indeed, we observed a significant decrease in actin staining within the vegetal half of the embryonic yolk sac, suggesting that niclosamide exposure decreased the ability

of the cortical actin network within the yolk sac to properly form – an effect which may have resulted in a loss of yolk sac integrity.

Interestingly, there did not appear to be any effect on actin networks in the cell mass, although there was a significant increase in average cell area following niclosamide exposure. Early cell divisions in the zebrafish embryo are regulated via maternal genes (Abrams and Mullins, 2009), during which the total volume of the embryo remains constant and each cell division results in progressively smaller cells (Kane and Kimmel, 1993; Langley et al., 2014). Therefore, it is possible that niclosamide exposure results in a systemic delay in development that impedes cell division and/or targets maternal transcripts responsible for cell division and yolk sac actin network formation. Given that the presence of the cortical actin network within the yolk sac prior to the MZT has not been well-studied, it is possible that decreased actin levels within the yolk sac were also due to a systemic delay in embryonic development. In addition, no significant effects on actin were observed following exposure of hESCs to non-cytotoxic concentrations of niclosamide, suggesting that a niclosamide-induced decrease in yolk sac actin networks within zebrafish embryos may be due to effects on processes absent within hESCs.

During early zebrafish embryogenesis, energy in the form of ATP is necessary to drive early developmental processes. This is particularly true for the MZT, where a pulse of energy is needed to drive the ATP-dependent degradation of maternal transcripts (DeRenzo and Seydoux, 2004; Dutta and Sinha, 2017). The ATP responsible for driving the MZT is produced through the metabolism of lipid droplets present in the blastodisc (cell-mass), and inhibition of lipolysis results in delays to developmental processes including epiboly and the MZT (Dutta and Sinha, 2017). Interestingly, whole-embryo profiles of non-polar metabolites and lipids within niclosamide-exposed embryos – either before (3 hpf) or after (5 hpf) the initiation of the MZT – were not significantly different relative to vehicle controls. Therefore, these results suggest that niclosamide-induced developmental delay may not be mediated through disruption of lipid metabolism.

During early zebrafish development, the translation of maternally-supplied transcripts is essential to produce proteins involved in early developmental processes, including several transcription factors involved in zygotic genome activation (Abrams and Mullins, 2009; Harvey et al., 2013; Langley et al., 2014; Lee et al., 2013). When maternal transcripts are deposited in the embryo following fertilization, these transcripts are maintained in an inactive state until needed for the translation of embryonic proteins (Harvey et al., 2013; Langley et al., 2014; Lee et al., 2013). Interestingly, blocking the activation of maternal mRNA prevents the activation of most zygotic genes as well as progression of epiboly (Aanes et al., 2011). In addition to mRNA, translation also requires functioning ribosomes, amino acids, and nucleotides (Putzer and Laalami, 2013). Following niclosamide exposure, levels of L-amino acids – metabolites specific to the aminoacyl-tRNA biosynthesis pathway – were significantly altered within whole embryos. In addition, the aminoacyl-tRNA biosynthesis pathway was the most significantly altered pathway in niclosamide exposed embryos following metabolomic analysis. During translation, the aminoacyl-tRNA biosynthesis pathway is required for supplying the ribosome with the correct amino acids to generate polypeptides (Ibba and Soll, 2000). Given the necessity of aminoacyl-tRNA in

translation and the importance of maternal mRNA translation for driving the MZT, epiboly, and embryonic development, our results suggest that niclosamide may be interfering with the production of maternal proteins, resulting in a cascade of downstream effects and developmental delays.

When differential expression analysis was performed on embryos demonstrating delayed maternal protein degradation and delayed zygotic genome activation (Vliet et al., 2018), we found that exposure to niclosamide resulted in significant and widespread alterations to the embryonic transcriptome. When compared to time-matched vehicle controls (2–5 hpf), 1,526 transcripts were significantly altered (671 and 855 transcripts were increased and decreased, respectively). Interestingly, when niclosamide-exposed embryos were compared to stage-matched vehicle controls (2–3 hpf), only 96 transcripts were significantly altered (85 and 11 transcripts were increased and decreased, respectively). Overall, these transcriptional responses suggest that niclosamide-exposed embryos are transcriptionally more like 3-hpf control embryos, further supporting the hypothesis that niclosamide exposure results in systemic delays to embryonic development. In addition, when differentially altered transcripts were categorized by maternal or zygotic, most maternal transcripts were increased relative to vehicle controls, while all zygotic transcripts were decreased relative to vehicle controls. These results are consistent with our previous studies and further support the hypothesis that exposure to niclosamide during this developmental window may interfere with the MZT, leading to decreased degradation of maternal proteins along with decreased production of zygotic transcripts.

When differentially expressed transcripts were further evaluated by DAVID and KEGG, the spliceosome pathway and transcriptional processes were the most statistically significant groups based on time-matched comparisons, and the ribosomal pathway and translational processes were the most statistically significant groups for stage-matched comparisons. These results are consistent with the hypothesis that niclosamide exposure may be delaying the MZT and causing a systemic delay in development by disrupting the translation of maternally-supplied mRNAs and preventing the successful transcription of zygotic genes, potentially through inhibition of the ribosomal machinery. The translation of proteins from maternal mRNA requires both functioning ribosomes as well as aminoacyl-tRNA and, during translation, tRNA present in the cytosol binds to free amino acids, becoming aminoacyl-tRNA. As the aminoacyltRNA biosynthesis pathway was significantly altered following niclosamide exposure, and our mRNA-sequencing data indicated that niclosamide may be altering translation through a ribosomal pathway, we investigated total levels of tRNA and rRNA. No significant alterations in the relative abundance of rRNA of tRNA were observed across either treatment condition or timepoint, suggesting that niclosamide is not directly impacting the synthesis or recycling of these RNA species. Instead of directly impacting tRNA or rRNA, these data support the hypothesis that niclosamide may be interfering with the ability of tRNA to bind amino acid and complete protein translation.

The aminoacylation of tRNAs with amino acids is catalyzed by aminoacyl-tRNA synthetases (AARSs), enzymes that are responsible for attaching the correct amino acid to the tRNA (Rajendran et al., 2018). Given the key role of AARS is this process, the enzyme provides a potential macromolecular target and molecular initiating event (MIE) for

niclosamide within zebrafish embryos. Within vertebrates, several different AARSs are present and the accurate recognition of the correct amino acid and tRNA is different for each enzyme. Since different amino acids have different functional groups, the enzyme for each amino acid has a different binding pocket (Rajendran et al., 2018). This difference in binding pocket provides a potential explanation as to why alterations in the relative abundance of free amino acids following niclosamide exposure was limited to a few amino acids; however, further research is needed to validate this hypothesis.

In conclusion, this study showed that (1) niclosamide exposure during early zebrafish embryogenesis resulted in a decrease in yolk sac integrity with a concomitant decrease in the presence of yolk sac actin networks and increase in cell size; (2) within whole embryos, niclosamide exposure did not alter non-polar metabolites and lipids, but significantly altered amino acids specific to aminoacyl-tRNA biosynthesis; (3) niclosamide significantly altered transcripts related to translation, transcription, and mRNA processing pathways; and (4) niclosamide did not significantly alter levels of rRNA and tRNA. Overall, our data suggest that niclosamide may be causing a systemic delay in embryonic development by disrupting the translation of maternally-supplied mRNAs, an effect that may be mediated through disruption of aminoacyl-tRNA biosynthesis. This study highlights the utility of the zebrafish embryo as a model for the identification of novel mechanisms of action.

Supplementary Material

Refer to Web version on PubMed Central for supplementary material.

Acknowledgements

This work was supported by UCR's NRSA T32 Training Program (T32ES018827), as well as a National Institutes of Health grant [R01ES027576] and the USDA National Institute of Food and Agriculture Hatch Project [1009609] to D.C.V.

References

Aanes H, Winata CL, Lin CH, Chen JP, Srinivasan KG, Lee SGP, Lim AYM, Hajan HS, Collas P, Bourque G, et al. (2011). Zebrafish mRNA sequencing deciphers novelties in transcriptome dynamics during maternal to zygotic transition. Genome Res. 21, 1328–1338. [PubMed: 21555364]

Abrams EW, and Mullins MC (2009). Early zebrafish development: It's in the maternal genes. Curr. Opin. Genet. Dev 19, 396–403. [PubMed: 19608405]

Andrews P, Thyssen J, and Lorke D (1982). The biology and toxicology of molluscicides, Bayluscide. Pharmacol. Ther 19, 245–295. [PubMed: 6763710]

Balgi AD, Fonseca BD, Donohue E, Tsang TCF, Lajoie P, Proud CG, Nabi IR, and Roberge M (2009). Screen for Chemical Modulators of Autophagy Reveals Novel Therapeutic Inhibitors of mTORC1 Signaling. PLOS ONE 4, e7124. [PubMed: 19771169]

Broeckling CD, Afsar FA, Neumann S, Ben-Hur A, and Prenni JE (2014). RAMClust: A Novel Feature Clustering Method Enables Spectral-Matching-Based Annotation for Metabolomics Data. Anal. Chem 86, 6812–6817. [PubMed: 24927477]

Cairns DM, Boorgu DSSK, Levin M, and Kaplan DL (2018). Niclosamide rescues microcephaly in a humanized in vivo model of Zika infection using human induced neural stem cells. Biol. Open 7, bio031807. [PubMed: 29378701]

Chen M, Wang J, Lu J, Bond MC, Ren X-R, Lyerly HK, Barak LS, and Chen W (2009). The Anti-Helminthic Niclosamide Inhibits Wnt/Frizzled1 Signaling. Biochemistry 48, 10267–10274. [PubMed: 19772353]

Chen W, Mook RA, Premont RT, and Wang J (2017). Niclosamide: Beyond an antihelminthic drug. Cell. Signal 41, 89–96. [PubMed: 28389414]

Cheng JC, Miller AL, and Webb SE (2004). Organization and function of microfilaments during late epiboly in zebrafish embryos. Dev. Dyn 231, 313–323. [PubMed: 15366008]

Dennis G, Sherman BT, Hosack DA, Yang J, Gao W, Lane HC, and Lempicki RA (2003). DAVID: Database for Annotation, Visualization, and Integrated Discovery. Genome Biol 4(5), P3. [PubMed: 12734009]

DeRenzo C, and Seydoux G (2004). A clean start: degradation of maternal proteins at the oocyte-to-embryo transition. Trends Cell Biol. 14, 420–426. [PubMed: 15308208]

Domalaon R, Silva PMD, Kumar A, Zhanel GG, and Schweizer F (2019). The Anthelmintic Drug Niclosamide Synergizes with Colistin and Reverses Colistin Resistance in Gram-Negative Bacilli. Antimicrob. Agents Chemother 63, e02574–18. [PubMed: 30917988]

Duffie R, and Bourc'his D (2013). Chapter Nine - Parental Epigenetic Asymmetry in Mammals In Current Topics in Developmental Biology, Heard E, ed. (Academic Press), pp. 293–328.

Dunn WB, Broadhurst D, Begley P, Zelena E, Francis-McIntyre S, Anderson N, Brown M, Knowles JD, Halsall A, Haselden JN, et al. (2011). Procedures for large-scale metabolic profiling of serum and plasma using gas chromatography and liquid chromatography coupled to mass spectrometry. Nat. Protoc 6, 1060–1083. [PubMed: 21720319]

Dutta A, and Sinha DK (2017). Zebrafish lipid droplets regulate embryonic ATP homeostasis to power early development. Open Biol. 7, 170063. [PubMed: 28679548]

Environmental Protection Agency, United States. (1999). Niclosamide. Prevention, Pesticides, and Toxic Substances R.E.D Facts. EPA-738-F99–013, 1–9.

Espinosa-Aguirre JJ, Reyes RE, and Cortinas de Nava C (1991). Mutagenic activity of 2 chloro-4-nitroaniline and 5-chlorosalicylic acid in Salmonella typhimurium: two possible metabolites of niclosamide. Mutat. Res. Lett 264, 139–145.

Gallicano GI (2001). Composition, Regulation, and Function of the Cytoskeleton in Mammalian Eggs and Embryos. Front. Biosci 6, 1089–1108.

Harvey SA, Sealy I, Kettleborough R, Fenyes F, White R, Stemple D, and Smith JC (2013). Identification of the zebrafish maternal and paternal transcriptomes. Dev. Camb. Engl 140, 2703–2710.

Huang DW, Sherman BT, and Lempicki RA (2009a). Bioinformatics enrichment tools: paths toward the comprehensive functional analysis of large gene lists. Nucleic Acids Res. 37, 1–13. [PubMed: 19033363]

Huang DW, Sherman BT, and Lempicki RA (2009b). Systematic and integrative analysis of large gene lists using DAVID bioinformatics resources. Nat. Protoc 4, 44–57. [PubMed: 19131956]

Ibba M, and Soll D (2000). Aminoacyl-tRNA synthesis. Annu. Rev. Biochem 69, 617–650. [PubMed: 10966471]

Imperi F, Massai F, Pillai CR, Longo F, Zennaro E, Rampioni G, Visca P, and Leoni L(2013). New Life for an Old Drug: The Anthelmintic Drug Niclosamide Inhibits Pseudomonas aeruginosa Quorum Sensing. Antimicrob. Agents Chemother 57, 996–1005. [PubMed: 23254430]

Jin Y, Lu Z, Ding K, Li J, Du X, Chen C, Sun X, Wu Y, Zhou J, and Pan J (2010). Antineoplastic Mechanisms of Niclosamide in Acute Myelogenous Leukemia Stem Cells: Inactivation of the NF-B Pathway and Generation of Reactive Oxygen Species. Cancer Res. 70, 2516–2527. [PubMed: 20215516]

Kane DA, and Kimmel CB (1993). The zebrafish midblastula transition. Development 119, 447–456. [PubMed: 8287796]

Keller R, Davidson LA, and Shook DR (2003). How we are shaped: the biomechanics of gastrulation. Differ. Res. Biol. Divers 71, 171–205.

Kimmel CB, Ballard WW, Kimmel SR, Ullmann B, and Schilling TF (1995). Stages of embryonic development of the zebrafish. Dev. Dyn 203, 253–310. [PubMed: 8589427]

Langley AR, Smith JC, Stemple DL, and Harvey SA (2014). New insights into the maternal to zygotic transition. Development 141, 3834–3841. [PubMed: 25294937]

Lee MT, Bonneau AR, Takacs CM, Bazzini AA, DiVito KR, Fleming ES, and Giraldez AJ (2013). Nanog, Pou5f1 and SoxB1 activate zygotic gene expression during the maternal-to-zygotic transition. Nature 503, 360–364. [PubMed: 24056933]

Lepage SE, and Bruce AEE (2010). Zebrafish epiboly: mechanics and mechanisms. Int. J. Dev. Biol 54, 1213–1228. [PubMed: 20712002]

Li L, Lu X, and Dean J (2013). The Maternal to Zygotic Transition in Mammals. Mol. Aspects Med 34, 919–938. [PubMed: 23352575]

Li Y, Li P-K, Roberts MJ, Arend RC, Samant RS, and Buchsbaum DJ (2014). Multi-targeted therapy of cancer by niclosamide: A new application for an old drug. Cancer Lett. 349, 8–14. [PubMed: 24732808]

Li Z, Brecher M, Deng Y-Q, Zhang J, Sakamuru S, Liu B, Huang R, Koetzner CA, Allen CA, Jones SA, et al. (2017). Existing drugs as broad-spectrum and potent inhibitors for Zika virus by targeting NS2B-NS3 interaction. Cell Res. 27, 1046–1064. [PubMed: 28685770]

Liu Y, Luo X, Shan H, Fu Y, Gu Q, Zheng X, Dai Q, Xia F, Zheng Z, Liu P, et al. (2019). Niclosamide Triggers Non-Canonical LC3 Lipidation. Cells 8(3), 248.

Lu D, Ma Z, Zhang T, Zhang X, and Wu B (2016). Metabolism of the anthelmintic drug niclosamide by cytochrome P450 enzymes and UDP-glucuronosyltransferases: metabolite elucidation and main contributions from CYP1A2 and UGT1A1. Xenobiotica 46, 1–13. [PubMed: 26068521]

MacLean B, Tomazela DM, Shulman N, Chambers M, Finney GL, Frewen B, Kern R, Tabb DL, Liebler DC, and MacCoss MJ (2010). Skyline: an open source document editor for creating and analyzing targeted proteomics experiments. Bioinforma. Oxf. Engl 26, 966–968.

Mook RA, Wang J, Ren X-R, Piao H, Lyerly HK, and Chen W (2019). Identification of novel triazole inhibitors of Wnt/β-catenin signaling based on the Niclosamide chemotype. Bioorg. Med. Chem. Lett 29, 317–321. [PubMed: 30551901]

Newton PT (2019). New insights into niclosamide action: autophagy activation in colorectal cancer. Biochem. J 476, 779–781. [PubMed: 30842311]

Pan J-X, Ding K, and Wang C-Y (2012). Niclosamide, an old antihelminthic agent, demonstrates antitumor activity by blocking multiple signaling pathways of cancer stem cells. Chin. J. Cancer 31, 178–184. [PubMed: 22237038]

Prather GR, MacLean JA, Shi M, Boadu DK, Paquet M, and Hayashi K (2016). Niclosamide As a Potential Nonsteroidal Therapy for Endometriosis That Preserves Reproductive Function in an Experimental Mouse Model. Biol. Reprod 95, 74–74.

Putzer H, and Laalami S (2013) Regulation of the Expression of Aminoacyl-tRNA Synthetases and Translation Factors. Landes Bioscience. RNA. https://www.ncbi.nlm.nih.gov/books/NBK6026/

Raheem KA, El-Gindy H, and Al-Hassan J (1980). Interrelationship of molluscicidal concentration and temperature on the respiration of Bulinus truncatus. Hydrobiologia 74, 11–15.

Rajendran V, Kalita P, Shukla H, Kumar A, and Tripathi T (2018). Aminoacyl-tRNA synthetases: Structure, function, and drug discovery. Int. J. Biol. Macromol 111, 400–414. [PubMed: 29305884]

Ren X, Duan L, He Q, Zhang Z, Zhou Y, Wu D, Pan J, Pei D, and Ding K (2010). Identification of Niclosamide as a New Small-Molecule Inhibitor of the STAT3 Signaling Pathway. ACS Med. Chem. Lett 1, 454–459. [PubMed: 24900231]

Schymanski EL, Jeon J, Gulde R, Fenner K, Ruff M, Singer HP, and Hollender J(2014). Identifying Small Molecules via High Resolution Mass Spectrometry: Communicating Confidence. Environ. Sci. Technol20144842097–2098.

Sha Q-Q, Zhang J, and Fan H-Y (2019). A story of birth and death: mRNA translation and clearance at the onset of maternal-to-zygotic transition in mammals. Biol. Reprod. ioz012, 10.1093/biolre/ioz012.

Solnica-Krezel L (2005). Conserved Patterns of Cell Movements during Vertebrate Gastrulation. Curr. Biol 15, R213–R228. [PubMed: 15797016]

Solnica-Krezel L, and Driever W (1994). Microtubule arrays of the zebrafish yolk cell: organization and function during epiboly. Development 120, 2443–2455. [PubMed: 7956824]

Suliman MA, Zhang Z, Na H, Ribeiro ALL, Zhang Y, Niang B, Hamid AS, Zhang H, Xu L, and Zuo Y (2016). Niclosamide inhibits colon cancer progression through downregulation of the Notch

pathway and upregulation of the tumor suppressor miR-200 family. Int. J. Mol. Med 38, 776–784. [PubMed: 27460529]

Sumner LW, Amberg A, Barrett D, Beale MH, Beger R, Daykin CA, Fan TW-M, Fiehn O, Goodacre R, Griffin JL, et al. (2007). Proposed minimum reporting standards for chemical analysis. Metabolomics 3, 211–221. [PubMed: 24039616]

Tao H, Zhang Y, Zeng X, Shulman GI, and Jin S (2014). Niclosamide ethanolamine– induced mild mitochondrial uncoupling improves diabetic symptoms in mice. Nat. Med 20, 1263–1269. [PubMed: 25282357]

Tharmalingam N, Port J, Castillo D, and Mylonakis E (2018). Repurposing the anthelmintic drug niclosamide to combat Helicobacter pylori. Sci. Rep 8, 3701. [PubMed: 29487357]

Tran UT, and Kitami T (2019). Niclosamide activates the NLRP3 inflammasome by intracellular acidification and mitochondrial inhibition. Commun. Biol 2, 2. [PubMed: 30740538]

Vliet SM, Dasgupta S, and Volz DC (2018). Niclosamide Induces Epiboly Delay During Early Zebrafish Embryogenesis. Toxicol. Sci 1;166(2):306–317. doi: 10.1093/toxsci/kfy214. [PubMed: 30165700]

Weinbach E, and Garbus J (1969). Mechanism of action of reagents that uncouple oxidative phosphorylation. Nature 221, 1016–1018. [PubMed: 4180173]

Xu M, Lee EM, Wen Z, Cheng Y, Huang W-K, Qian X, Tcw J, Kouznetsova J, Ogden SC, Hammack C, et al. (2016). Identification of small-molecule inhibitors of Zika virus infection and induced neural cell death via a drug repurposing screen. Nat. Med 22, 1101–1107. [PubMed: 27571349]

Yartseva V, and Giraldez AJ (2015). The maternal-to-zygotic transition during vertebrate development: a model for reprogramming. Curr. Top. Dev. Biol 113, 191–232. [PubMed: 26358874]

Yorke RE, and Turton JA (1974). Effects of fasciolicidal and anti-cestode agents on the respiration of isolated Hymenolepis mitochondria. Z. Fur Parasitenkd. 45, 1–10.

Highlights

- Niclosamide decreases the presence of yolk sac actin networks.
- Niclosamide alters amino acids specific to aminoacyl-tRNA biosynthesis.
- Niclosamide alters transcripts related to mRNA processing pathways.
- Niclosamide does not significantly alter levels of rRNA and tRNA.

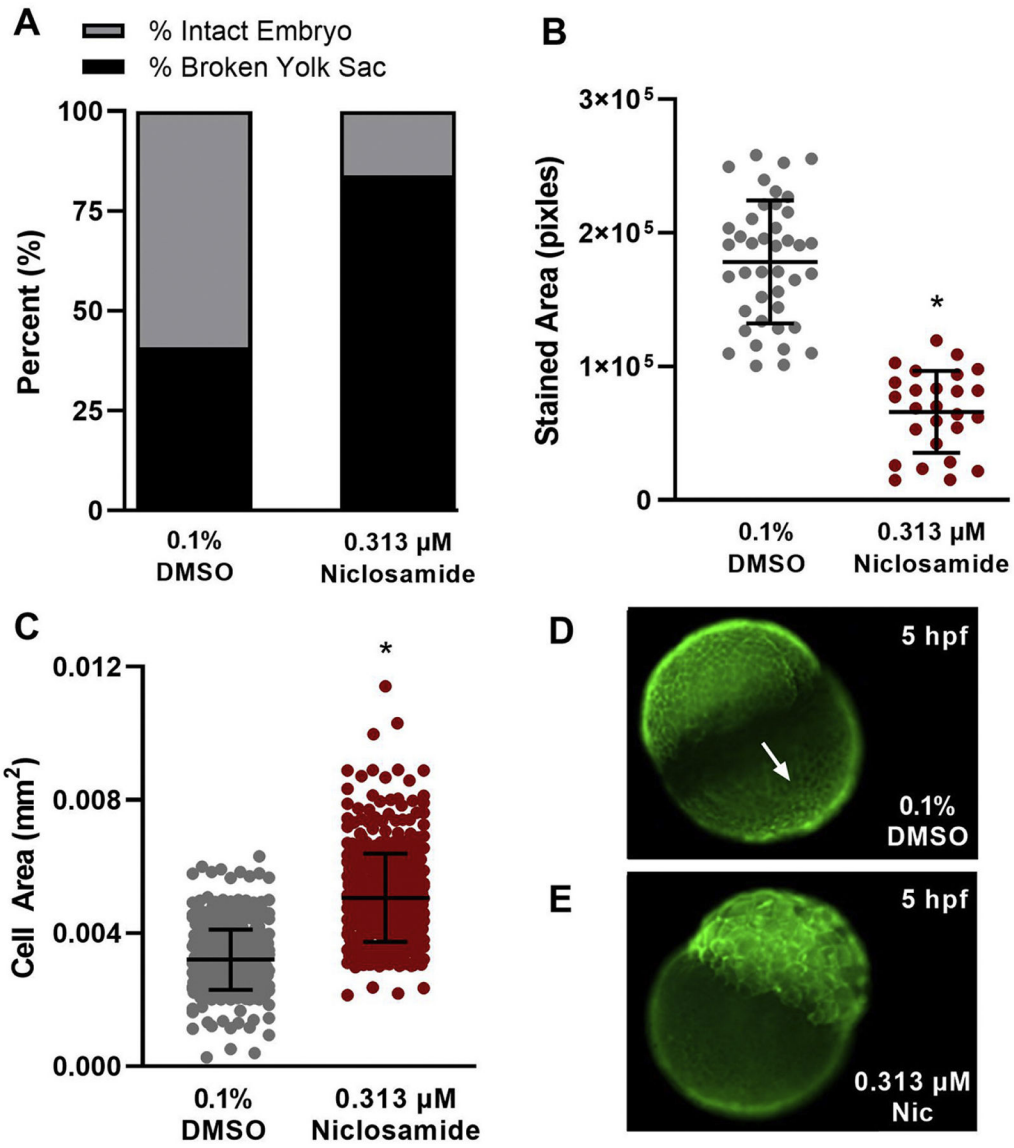

Figure 1.

Niclosamide exposure alters yolk sac integrity, the presence of yolk sac cortical actin networks, and cell size in the embryonic blastodisc within 5-hpf embryos. Niclosamide exposure decreases embryonic yolk sac integrity in 5-hpf embryos (A), actin present in the embryonic yolk sac of intact embryos (B), and the size of cells present in the embryonic blastodisc in 5 hpf embryos (C). Representative images of vehicle- (0.1% DMSO) and niclosamide-treated (0.313 µM) embryos stained with phalloidin (D, E). The cortical actin network is visible in the vegetal half of the embryonic yolk sac, indicated by the white arrow in panel D. Asterisk denotes $p < 0.05$.

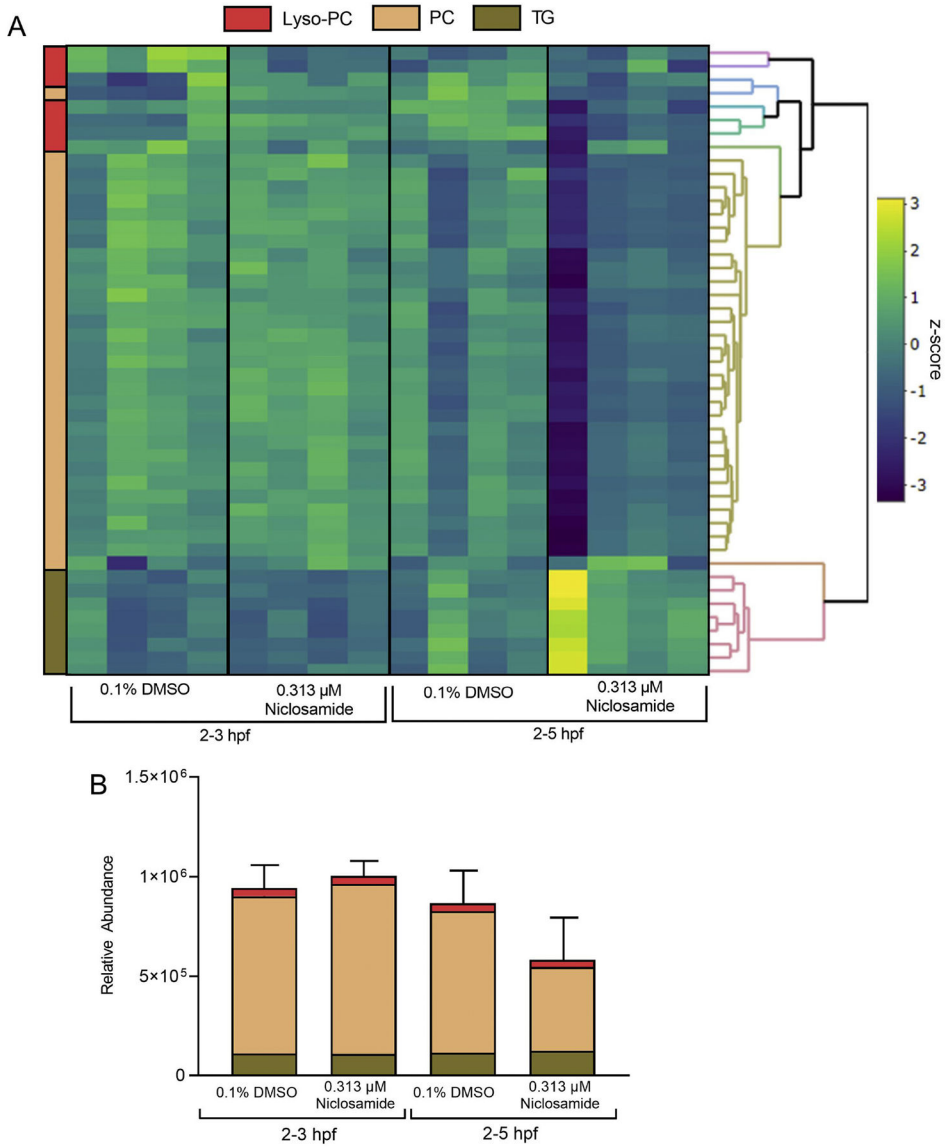

Figure 2.

Niclosamide exposure does not result in significant effects on the distribution and relative abundance of non-polar metabolites. (A) No significant differences ($p > 0.05$) were observed among the 47 identified non-polar metabolites following niclosamide exposure. (B) Following niclosamide treatment, there were no significant differences ($p > 0.05$) in the relative abundance of identified lipid species nor the proportion of different lipid classes relative to vehicle controls. Lyso-PC = Lysophosphatidylcholine; PC = Phosphatidylcholine; and TG = Triglycerides.

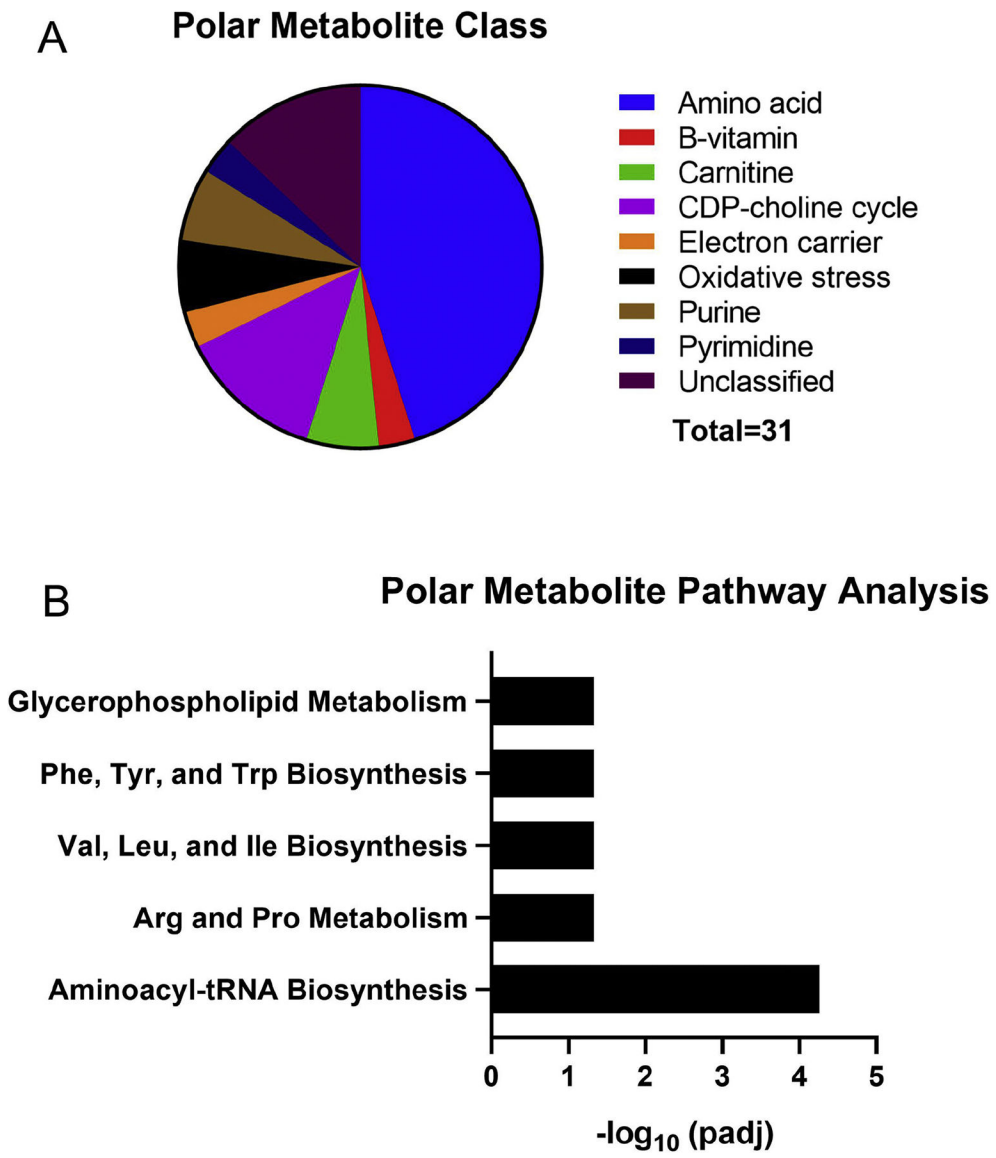

Figure 3.

Thirty-one polar metabolites were significantly altered by niclosamide exposure. (A) Of the 31 significantly altered polar metabolites, the majority were annotated within the “amino acids” group. (B) Pathways significantly affected by niclosamide exposure were identified within MetaboAnalyst using a Fisher’s Exact p-value < 0.05.

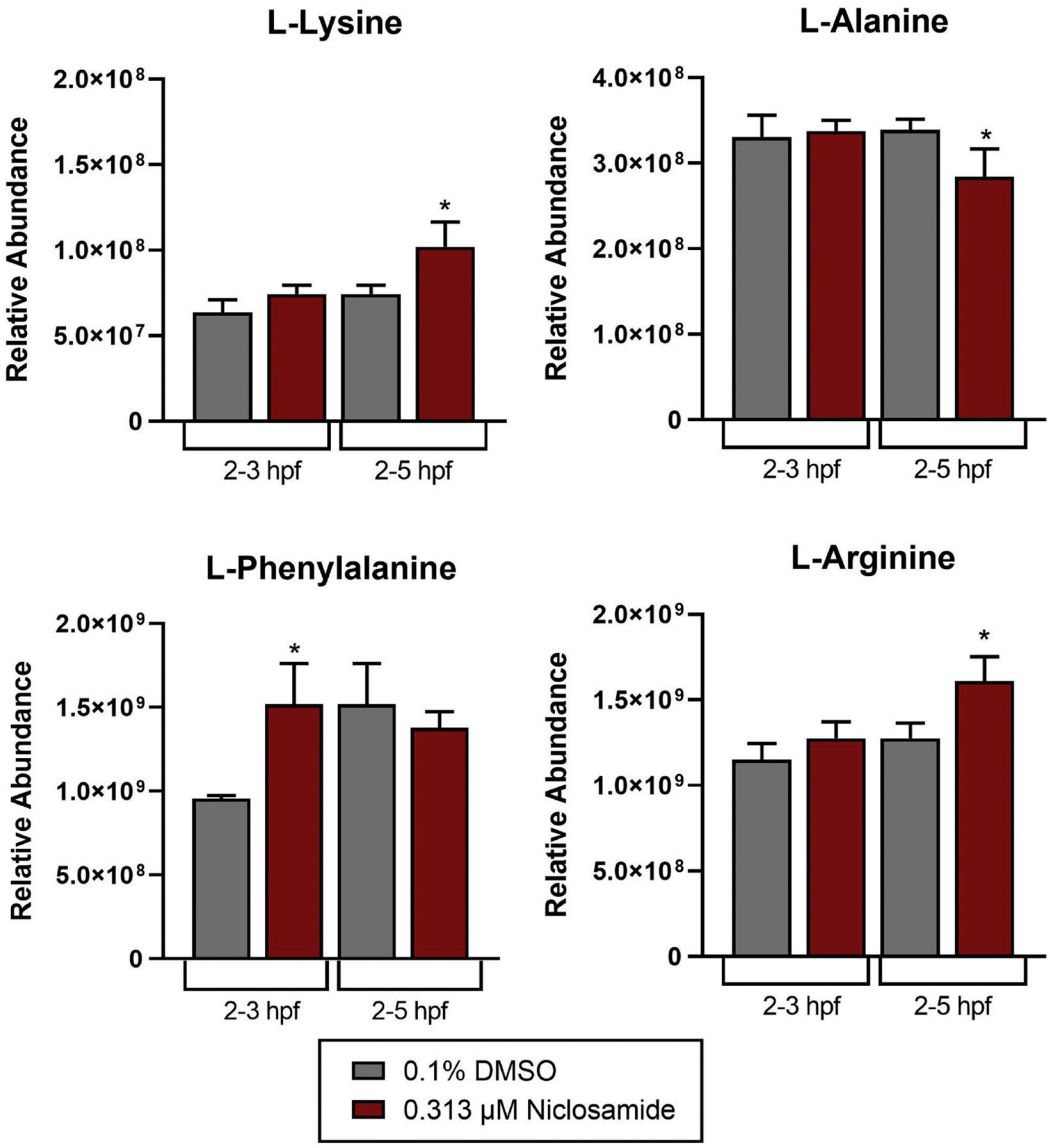

Figure 4.

Among the significantly altered metabolites specific to the aminoacyl-tRNA biosynthesis pathway, there were significant treatment-related effects on the relative abundance of L-amino acids (L-phenylalanine, L-lysine, L-alanine, and L-arginine) following niclosamide exposure relative to time-matched vehicle controls. Asterisk denotes $p < 0.05$.

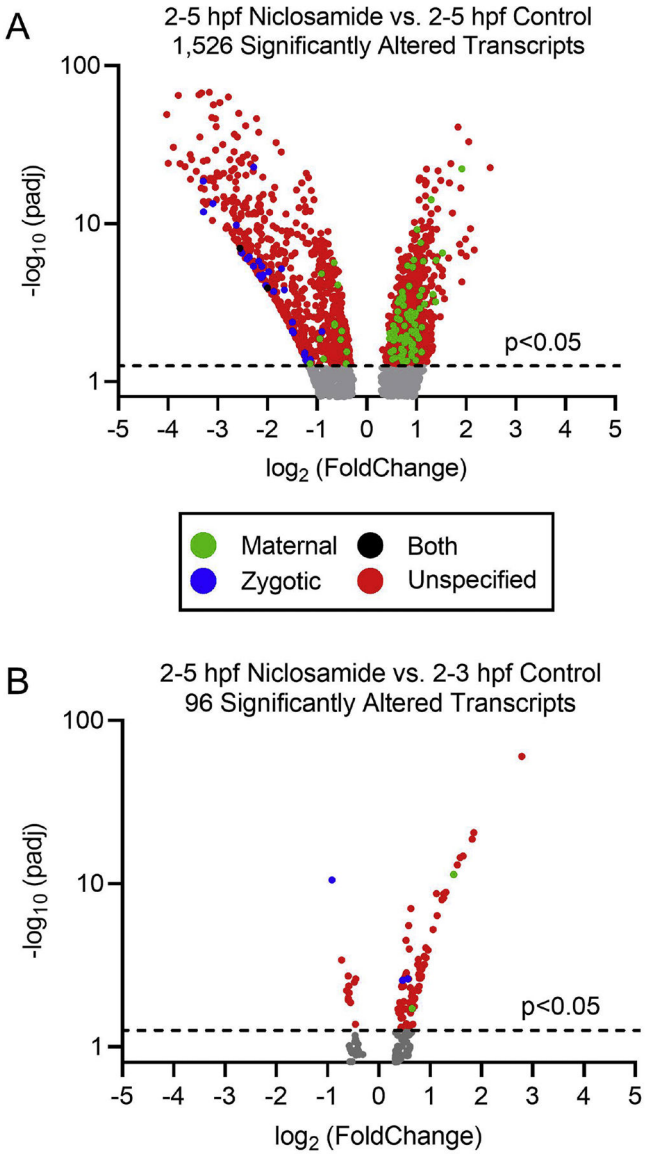

Figure 5.

Exposure to 0.313 μM niclosamide from 2–5 hpf resulted in widespread alterations to transcript levels relative to time-matched (5 hpf) vehicle controls (A), an impact that was less severe relative to stage-matched (3 hpf) vehicle controls (B).

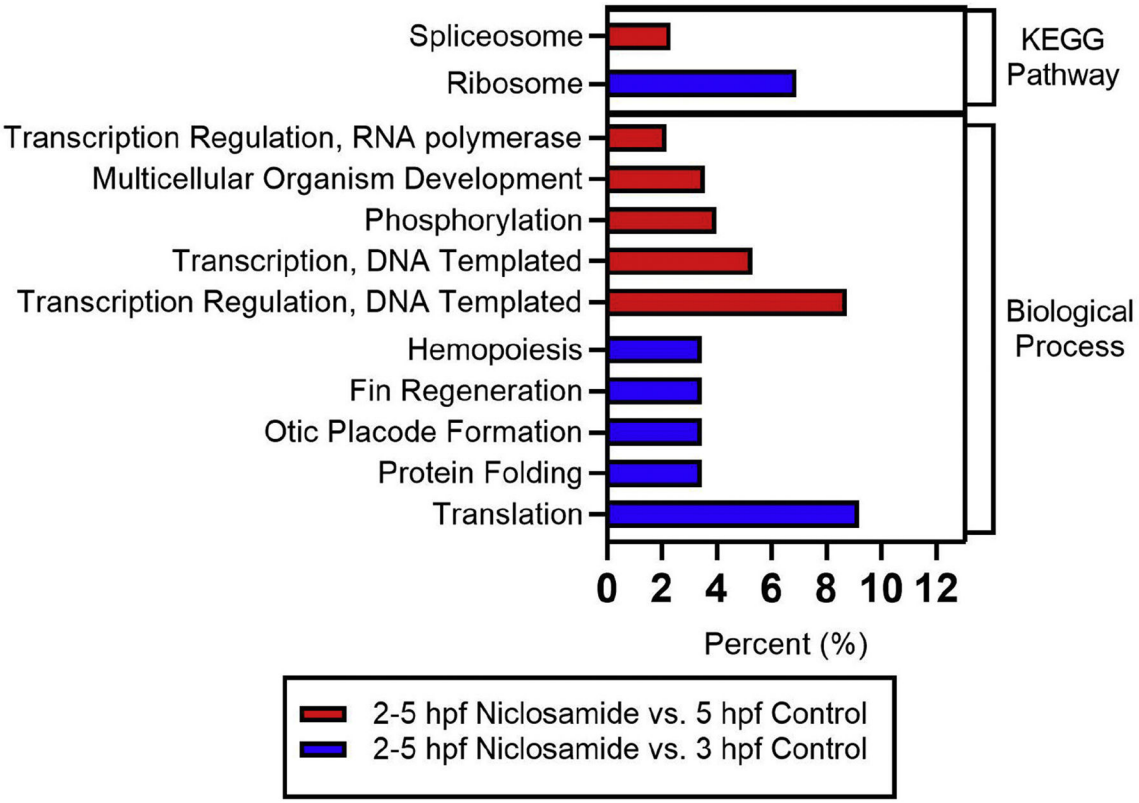

Figure 6.

Top KEGG pathways and DAVID biological processes identified following time-matched (2–5 hpf niclosamide vs. 2–5 hpf control) and stage-matched (2–5 hpf niclosamide vs. 2–3 hpf control) comparisons. Percent (%) indicates number of genes in data set per total genes in pathway.

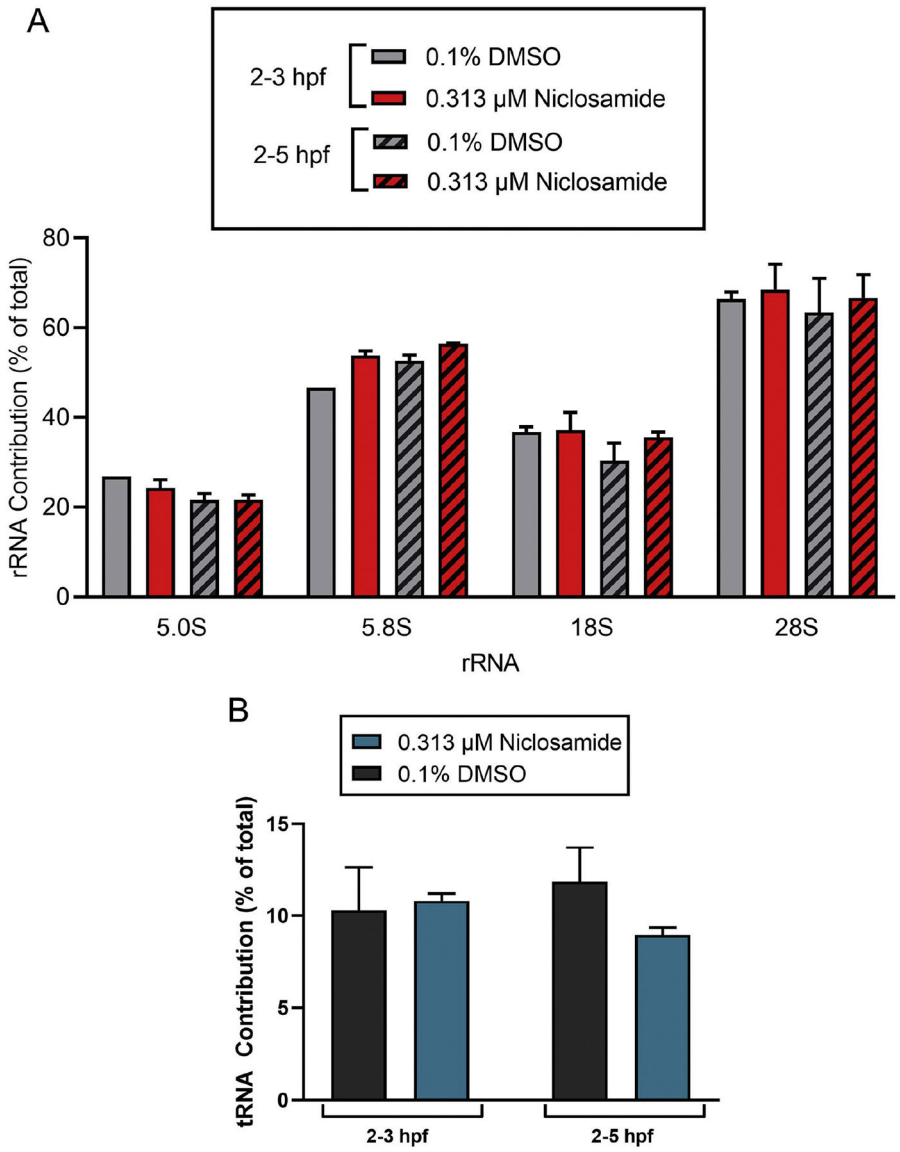

Figure 7.

Exposure to 0.313 µM niclosamide from 2–3 and 2–5 hpf does not result in significant alterations to (A) the percent contribution of ribosomal RNA (rRNA) and (B) the percent contribution of transfer RNA (tRNA) in zebrafish embryos. Percent (%) indicates the concentration of rRNA or tRNA relative to the total amount of RNA.